AGU PUBLICATIONS

Geophysical Research Letters

RESEARCH LETTER
10.1002/2017GL073421

Special Section:
Early Results: Juno at Jupiter

Key Points:
- A planetary-scale disturbance developed in the highest-speed Jupiter jet at 23.5°N latitude during October and November 2016
- Four "plumes" were involved in the outbreak moving with speeds between 155 and 175 m s^{-1}, the fastest features at cloud level
- Nonlinear numerical models reproduce the disturbance from the interaction between local sources (the plumes) and the zonal eastward jet

Supporting Information:
- Supporting Information S1

Correspondence to:
A. Sánchez-Lavega,
agustin.sanchez@ehu.eus

Citation:
Sánchez-Lavega, A., et al. (2017), A planetary-scale disturbance in the most intense Jovian atmospheric jet from JunoCam and ground-based observations, *Geophys. Res. Lett.*, *44*, 4679–4686, doi:10.1002/2017GL073421.

Received 18 MAR 2017
Accepted 12 APR 2017
Published online 25 MAY 2017

A planetary-scale disturbance in the most intense Jovian atmospheric jet from JunoCam and ground-based observations

A. Sánchez-Lavega[1], J. H. Rogers[2], G. S. Orton[3], E. García-Melendo[4], J. Legarreta[5], F. Colas[6], J. L. Dauvergne[7], R. Hueso[1], J. F. Rojas[1], S. Pérez-Hoyos[1], I. Mendikoa[1], P. Iñurrigarro[1], J. M. Gomez-Forrellad[4], T. Momary[3], C. J. Hansen[8], G. Eichstaedt[9], P. Miles[10], and A. Wesley[11]

[1]Departamento Física Aplicada I, Escuela de Ingeniería de Bilbao, Universidad del País Vasco UPV/EHU, Bilbao, Spain, [2]British Astronomical Association, London, UK, [3]Jet Propulsion Laboratory, Pasadena, California, USA, [4]Fundació Observatori Esteve Duran, Seva, Spain, [5]Sistemen Ingeniaritza eta Automatika Saila, Bilboko Ingeniaritza Eskola, Euskal Herriko Uniberstitatea UPV/EHU, Bilbao, Spain, [6]IMCCE, Observatoire de Paris, Paris, France, [7]S2P, Ciel et Espace, Paris, France, [8]Planetary Science Institute, Tucson, Arizona, USA, [9]Independent Scholar, Stuttgart, Germany, [10]Gemeye Observatory, Rubyvale, Queensland, Australia, [11]Astronomical Society of Australia, Murrumbateman, New South Wales, Australia

Abstract We describe a huge planetary-scale disturbance in the highest-speed Jovian jet at latitude 23.5°N that was first observed in October 2016 during the Juno perijove-2 approach. An extraordinary outburst of four plumes was involved in the disturbance development. They were located in the range of planetographic latitudes from 22.2° to 23.0°N and moved faster than the jet peak with eastward velocities in the range 155 to 175 m s^{-1}. In the wake of the plumes, a turbulent pattern of bright and dark spots (wave number 20–25) formed and progressed during October and November on both sides of the jet, moving with speeds in the range 100–125 m s^{-1} and leading to a new reddish and homogeneous belt when activity ceased in late November. Nonlinear numerical models reproduce the disturbance cloud patterns as a result of the interaction between local sources (the plumes) and the zonal eastward jet.

1. Introduction

Planetary-scale disturbances in Jupiter's atmosphere are the main source of the changes in the belt-zone albedo pattern and in the global appearance of the planet. There are two regions of Jupiter, the South Equatorial Belt (SEB) at planetographic latitude ~16°S and the North Temperate Belt southern component (NTBs) at latitude 23.5°N, that undergo such changes in a dramatic and somewhat similar manner [*Peek*, 1958; *Rogers*, 1995; *Sánchez-Lavega and Gómez*, 1996; *Sánchez-Lavega et al*., 2008]. They start from a similar single or multiple convective outbreak that manifests as a bright spot (at visual wavelengths) whose interaction with the sheared background winds forms a characteristic disturbance that propagates relative to the outbreak source, encircling the whole latitude in ~1–3 months, finally generating a new low-albedo band (a belt). We refer to these great disturbances as the SEBD and the NTBD, following previous works by *Sánchez-Lavega et al*. [1991, 2008] (see *Rogers* [2016] for the nomenclature of events at these latitudes). Just like the similar Great White Spot phenomena in Saturn's atmosphere [*Sánchez-Lavega et al*., 2017], these outbreak events give us information on the atmospheric dynamics and cloud and aerosol behavior over the pressure range in altitude from 0.01 to 5 bar.

A typical NTBD (plume outbreak and planetary-scale disturbance) starts at the latitude ~23.5°N on the peak of the most rapid Jovian jet at cloud tops (pressure level ~0.7 bar) as observed at visual wavelengths [*Rogers*, 1995; *Sánchez-Lavega et al*., 2008]. The jet peak velocity ranges from ~135 to 175 m s^{-1}, where this variability could be intrinsic or related to different altitudes of the tracers coupled to a possible vertical wind shear. The jet gradually accelerates before a NTBD outbreak, until it reaches almost the speed of the subsequent plumes [*Rogers et al*., 2006; *Sanchez-Lavega et al*., 2008]. The best studied events occurred in 1975 [*Rogers*, 1976; *Sánchez-Lavega and Quesada*, 1988], 1990 [*Sánchez-Lavega, et al*., 1991; *Rogers*, 1992; *García-Melendo et al*., 2005], and 2007 [*Sánchez-Lavega et al*., 2008; *Rogers and Mettig*, 2008]. The last NTBD before the present one occurred in April 2012 but was not well observed due to solar conjunction [*Rogers and Adamoli*, 2012]. Here we present a study of the 2016 outbreak that was exceptional since four plumes

were active in generating the disturbance, whereas in the last two well-studied events in 1990 and 2007 there were two plumes. In addition, this eruption took place shortly before the Juno spacecraft perijove-2 (PJ2) on 19 October.

2. Observations

For this study we used the following: (1) images obtained in the spectral range 0.38–1 μm with telescopes of 25–50 cm in diameter, from the Planetary Virtual Observatory and Laboratory (PVOL) database [*Hueso et al*., 2010, 2017a] and with telescopes from the Aula EspaZio Gela Observatory [*Sánchez-Lavega et al*., 2014]; (2) images obtained with PlanetCam "lucky imaging" camera that operates between 0.38 and 1.7 μm mounted on the 2.2 m telescope at Calar Alto Observatory in Spain [*Mendikoa et al*., 2016]; (3) JunoCam color image series [*Hansen et al*., 2014] obtained during perijove-2 approach between 11 and 14 October; (4) the 3 m planetary-dedicated NASA Infrared Telescope Facility (IRTF) using the SpeX imager (wavelengths 1.58, 1.64, 1.65, 2.16, 2.26, 3.42, 3.8, and 5.1 μm); and (5) the 1 m planetary-dedicated telescope at Pic-du-Midi Observatory (France) in the red range (0.6–1 μm). See supporting information for the list of contributors, databases, and methods used to analyze these images.

2.1. Pre-outbreak Clouds

Hubble Space Telescope (HST) maps of the cloud morphology obtained on 9–10 February 2016 show that northward of the jet peak in a conspicuous narrow band from latitudes 24.5° ± 0.2° to 25.5° ± 0.4°, the reflectivity at 275 nm was high relative to surroundings, but it was low in the 890 nm methane absorption band (OPAL program [*Simon et al*., 2015] (Figures S1 and S5 [*Hueso et al*., 2017b]). This suggests that this narrow band was a region depleted in high-altitude aerosols, with UV brightness due to Rayleigh scattering and methane band darkness due to gas absorption. We performed a preliminary analysis of photometrically calibrated PlanetCam images obtained before the outbreak on 19 May 2016 using nine filters from the UV (378 nm) to three near-infrared methane absorption bands (M2—727 nm, M3—890 nm, and YM—1.162 μm) and their adjacent continuums (Figure S2). Radiative transfer models for February 2016 show a particle-free stratosphere and upper troposphere with a haze deck located at 370 ± 100 mbar with optical thickness of τ_{haze} = 3.8 ± 0.6, above a cloud (τ_{cloud} = 6.0 ± 2.0) assumed to be located at the ammonia condensation level (~ 700 mbar) (see supporting information).

At 658 nm, the northern and southern parts of the jet, with cyclonic (latitude range 24° to 29°) and anticyclonic (19° to 23.5°) ambient vorticities, respectively, were turbulent and occupied by a pattern of spots at visible wavelengths, darker on the southern side where they showed a wavy appearance with some spatial periodicity (Figure S1). Color composite maps showed that the southern pattern was pale blue but at the jet and on the northern side the color was brown, denoting the effects of altitude differences and probably differences in the nature of chromophores at both sides of the jet (see supporting information).

2.2. Disturbance Outbreak: The Plumes

JunoCam images obtained between 11 and 14 October during the PJ2 approach phase (PJ2 was on 19 October) showed, at high phase angle and low resolution, bright and dark spots pertaining to the NTBs jet outbreak [*Rogers*, 2016] (Figure 1a). Four bright spots or "plumes" labeled as A, B, C, and D were sequentially captured as they came into view as the planet rotated (in section 2.3 we give estimates of the outbreak times). Their mutual separation ranged from ~27,000 km to 229,500 km (Figures 1b and 2). The brightest part of the plumes A and D (their "cores") had a size of 4700 km (east-west) and 3200 km (north-south), as measured on 19 October at 3.8 μm from IRTF images. The plumes were bright at 2.12 and 2.16 μm where molecular hydrogen absorption dominates and at 3.8 μm that senses altitude levels above the main upper cloud layer [*Irwin*, 2003]. However, they do not appear at 5.1 μm (Figure S3), sensitive to thermal infrared radiation from the interior, indicating that they had high opacity, consistent with the presence of thick clouds. Both aspects are in good agreement with the high cloud-altitude and high-opacity plumes quantitatively described in *Sánchez-Lavega et al*. [2008].

The plumes emerged in the anticyclonic southern flank of the undisturbed jet (Figure 3). Plume A was located at latitude +22.4° ± 0.7° and had a longitude drift rate of −4.2°/d in System I (SI) (speed 157.3 ± 1.1 m s^{-1} in System III or SIII) as retrieved from a simple linear fit (Figure 2). Throughout the paper, the velocities given in m s^{-1} take System III as reference (see supporting information for system definitions). Plume D was at

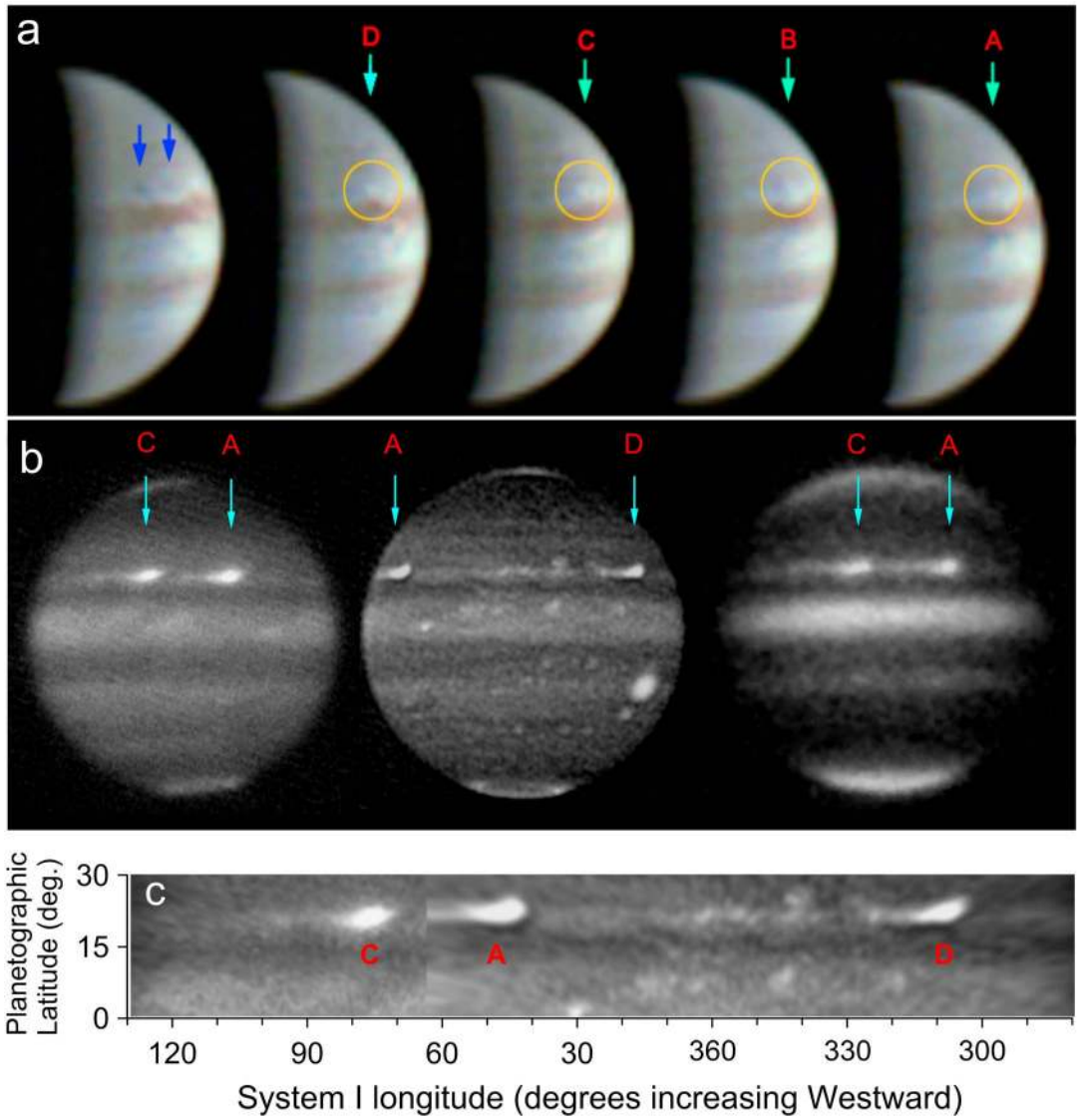

Figure 1. Images of the NTBD outbreak plumes: (a) JunoCam image series obtained on 14 October in SCET (UT at spacecraft, hh:mm:ss), from right to left: Image 085 (09:43:31), Image 089 (10:45:07), Image 091 (11:15:10), Image 113 (16:45:16), and Image 115 (17:15:20). The dark spots pertaining to the NTBD (blue arrows) and the four different plumes (A, B, C, and D) are marked by red arrows and circles, respectively. (b) SpeX IRTF images on 19 October showing plumes (A, C, and D) at wavelengths 3.8 μm (19:47:39 UT, left, and 17:50:27 UT, middle) and 2.12 μm (19:56:51, right). (c) Map showing the location of plumes C, A, and D from the series (Figure 1b).

+23.0° ± 1.0° and had a drift rate of −5.64°/d in SI (speed 176.4 ± 1.3 m s^{-1}). Plumes B and C showed a more complex behavior. The drift rate of these plumes suggests that a merger of B and C could have occurred, but it is also possible that one of them disappeared rapidly. Two motion solutions are possible, one extremely fast with drift rate −7.2°/d in SI (198.6 ± 2 m s^{-1}) never observed on Jupiter and the other with −4.8°/d in SI (166.5 ± 1.8 m s^{-1}) for the track of B plus C after 19 October (latitude +22.2° ± 0.8°). We adopt this second case for our wind profile and simulations, calling this plume C. Plumes C and D disappeared by the end of October upon arriving at the location of the chains of dark spots preceding them and located to the north of the jet (Figures 3 and 4), but A was alive until early November. The lifetimes of the plumes of about 1 month are typical of the NTBD phenomena [*Sánchez-Lavega et al.*, 1991, 2008].

2.3. The Planetary-Scale Disturbance

As observed in previous cases [*Sánchez-Lavega et al.*, 1991, 2008], each plume generated a wake consisting of a turbulent pattern of bright and dark spots that forms continuously on their westward side (i.e., following them) that progressed during October and November at both sides of the jet peak spanning a latitude

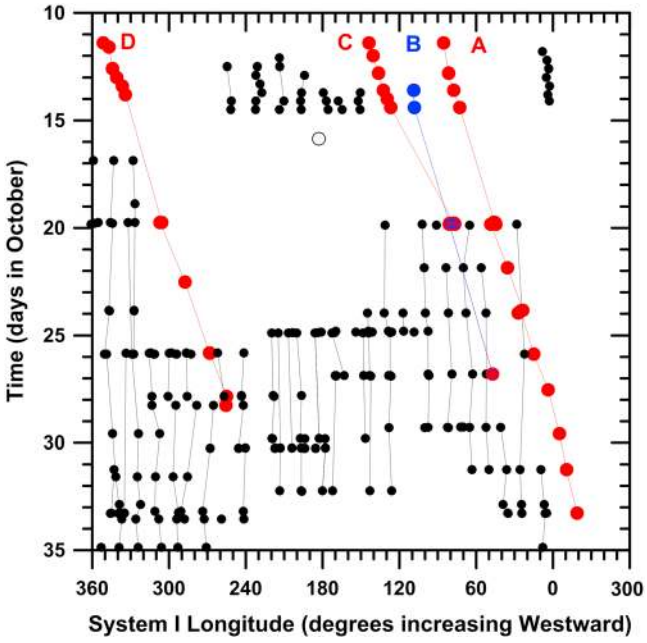

Figure 2. Drift rate in System I longitude of the features pertaining to the NTBD, tracked between 10 October and 4 November 2016. The plumes A, C, and D are identified by red dots. Plume B is the blue dot: it disappeared or merged with plume C. The dark dots indicate features forming the NTBD westward of the plumes. The lines identify the tracking of the features. Data from JunoCam images are for 11–14 October.

band from ~19° to 27°N (Figure 3) and being nearly stationary relative to System I (Figure 2). Pre-outbreak images from July and August 2016 show the NTB free of this pattern (images available on PVOL server; see supporting information). The turbulent pattern was formed by a chain of alternating irregular dark and bright features as observed at red continuum wavelengths, with an approximate wave number of 20–25 (wavelengths ~8000–10,000 km). The highest-resolution images (31 October to 6 November) showed the pattern of dark spots at latitude 24.5° ± 0.5°N in the cyclonic side of the pre-outbreak jet profile and bright arc-shaped filaments at 21.5° ± 0.5° in the pre-outbreak anticyclonic side (Figure 3). Each dark bright feature had a length of ~14,000 km, and its morphology, reflectivity in the visual, and radiance at short infrared wavelengths (1.58, 2.16, 3.8, and 5.1 μm, Figures 3 and S4) were consistent with descending motions in the cyclonic side (low cloud opacity and high radiances at 5.1 μm) and ascending motions in the bright arc-shaped side (high clouds and reflectivity at 2.16 μm). The mean speed of these features was nearly constant from ~21 to 26°N (Figure 4), and they formed a pattern reminiscent of the NEBs dark formations (hot spots), gyres, and EZn festoons, so they could be wave-induced features, as our numerical modeling suggests (see section 4). Tracking these features yielded speeds in the range 100–125 m s^{-1} relative to System III or ~−50 m s^{-1} relative to NTBs pre-outbreak jet peak speeds (Figures 2 and 3).

The first images of the plumes on 11–13 October by JunoCam showed that the long chain of dark spots westward of plumes B and C extended ~120° in longitude or 159,000 km. Assuming a relative speed of ~60 m s^{-1} between the plumes and the dark spot pattern, the outbreak of B or C or both probably occurred around 13–16 September. Similarly, on 19 October the disturbance pattern westward of plume D extended ~65° or 75,000 km indicating that its outbreak probably occurred on 4–8 October. The separation between plume D and the others was too large for one to have triggered the others, suggesting that an unknown process at a deeper level triggered multiple outbreaks within a short time span, as has been observed at previous outbreaks [*Sánchez-Lavega et al.*, 1991, 2008].

Once the plumes ceased their activity, the mixing of the features forming the disturbance, most probably generated by turbulence and wind shear, began to form a new North Temperate Belt. At the end of November a red and uniform belt was visible over the jet spanning a latitude range from 22.8° to 26.7°, but all was gray and turbulent on the poleward side from latitudes 26.7° to 32° (Figure S5). The equatorward latitude of the reddish belt edge (22.8°) is where the plumes emerged, whereas the northern edge corresponds to a latitude (26.7°) where the measurements of the velocity of the features pertaining to the disturbance (Figure 4) show a sudden change in their velocity. The white North Tropical Zone showed a long chain of narrow dark filaments tilted from latitudes 19.3° to 22.3° according to the ambient anticyclonic wind shear.

3. Disturbance Motions and Wind Profile

Jupiter's wind profile at the upper cloud level was measured in 2016 before the outbreak, using cloud automatic tracking on a large set of images and HST image pairs from February 2016 and also using ground-based

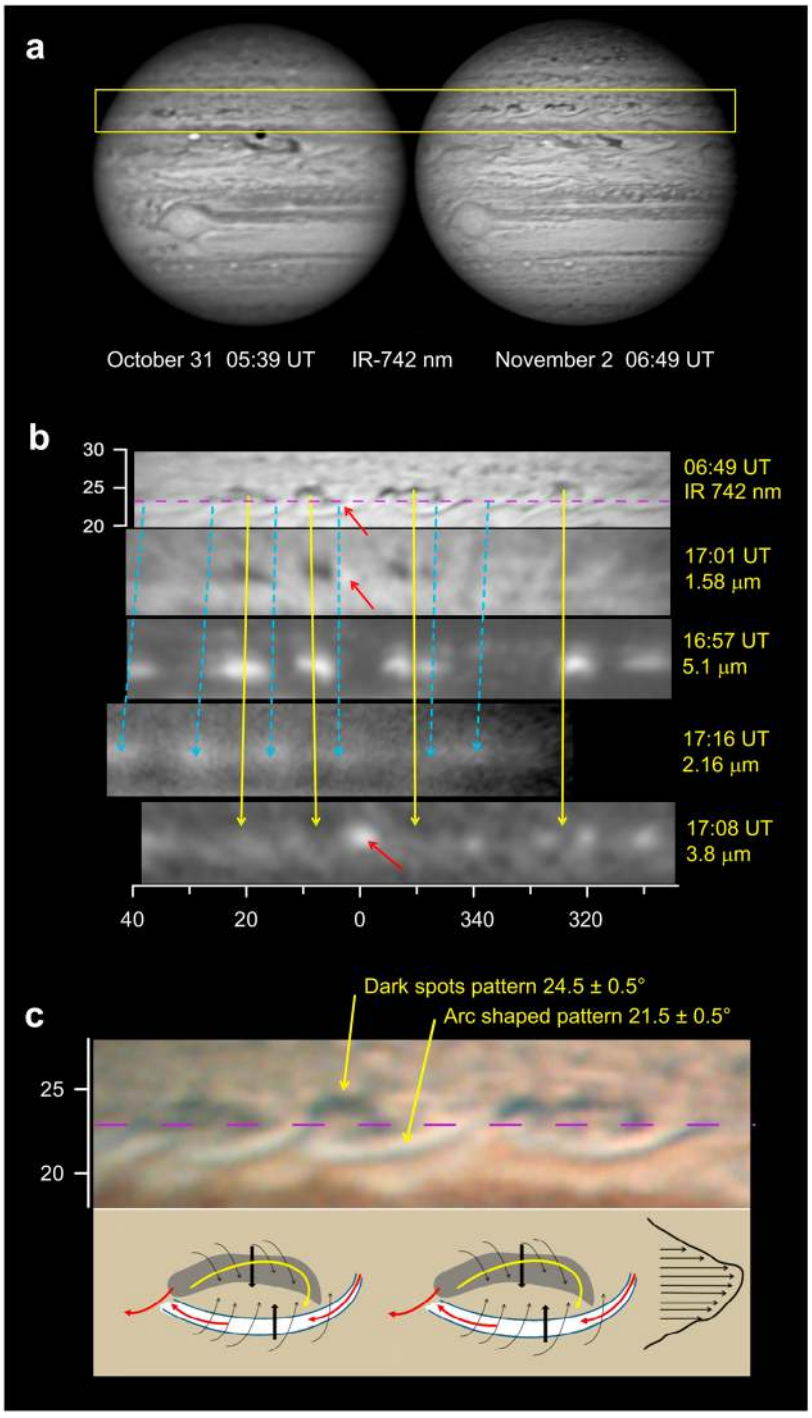

Figure 3. Images showing the features pertaining to the NTBD westward of the plumes: (a) Images acquired at the Pic-du-Midi Observatory obtained within the spectral range 0.742–1.0 μm showing the same region of the NTBD after 49 h, at the indicated days and times. (b) Strips maps of the NTBD on 2 November at the indicated times and wavelengths with longitude in System I and planetographic latitudes. Two families of features are shown, one at mean planetographic latitude 24.5° (identified by yellow arrows, cyclonic) and the other at 21.5° (identified by blue dashed arrows, anticyclonic). However, we note that some of the features in the 2.16 and 3.8 μm images may be unrelated to the NTBD. The red arrow identifies a particularly bright spot, probably transient, at 3.8 μm (high aerosol density). The residual of plume A is probably the weakly bright spot in the IR 742 nm filter at ~320° I (not present at other wavelengths). (c) Color enlargement showing the morphology of the first strip shown in Figure 3b. The cartoon shows a possible circulation for each dark spot—arc-shaped pair within the pre-outbreak meridionally sheared flow at right. The dashed violet line marks the location of the jet peak before the outbreak.

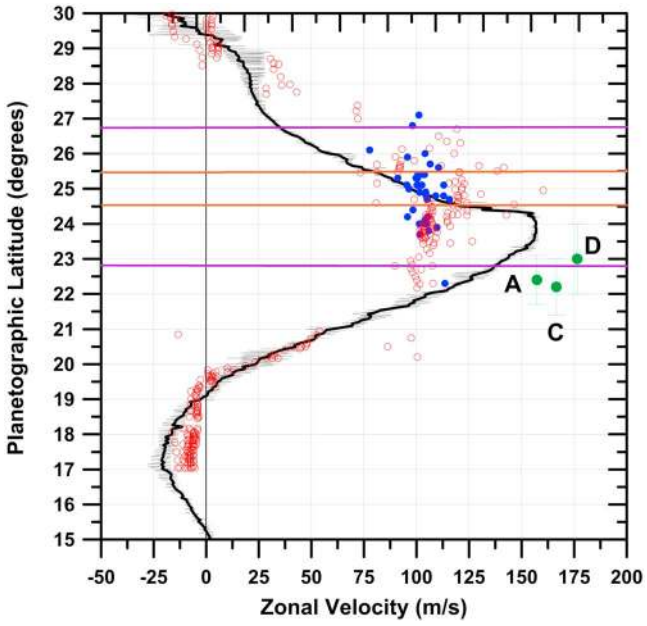

Figure 4. Meridional profile of the NTBs jet stream as measured using HST images on 9–10 February 2016 about 7–8 months before the outbreak (black curve with wind error measurement indicated [*Hueso et al.*, 2017b]). The velocity and location of the NTBD disturbance features are shown as dots: green for the plumes (A, C, and D), blue dots for long-term tracked features (dark and white spots, tracking for 5–10 days), and circles for all kind of features (tracking on Pic-du-Midi images for about 50 h using two methods). The NTBD data correspond to the period 11 October to 11 November 2016. The horizontal orange lines mark the limits of the pre-outbreak band that was bright in UV but dark in methane absorption at 890 nm (Figure S1). The horizontal purple lines mark the limits of the reddish band that formed when the NTBD activity ceased (Figure S5).

observations with small telescopes up to May 2016 [*Hueso et al.*, 2017b]. We use the NTBs HST jet profile as a reference for the motions and dynamics of the NTBD.

We have used cloud tracking in October and November 2016 to determine the motions of the features pertaining to the NTBD, covering the latitude range of the jet from 15°N to 30°N. Two methods have been used: (1) long-term tracking (typically 5 to 30 days) of the most conspicuous features, including the plumes and using a linear fit to the drift rate that gives the wind speed (Figure 2), and (2) tracking of individual features and supervised brightness correlation cloud tracking [*Hueso et al.*, 2009] on image pairs separated a maximum of 2 days on the highest-resolution images obtained at Pic-du-Midi Observatory from 30 October to 3 November. Both methods are complementary and show similar results. The first method provides fewer tracers, but the precision of the velocity determination is high (typically <3 m s^{-1}). The second one provides large numbers of tracers, but the precision is lower (~10 m s^{-1}).

In Figure 4 we compare the wind profile measured before the eruption and the velocities of the features pertaining to the NTBD. As stated above, the plumes were located ~1° south of the previous jet peak and moved faster than it. Most features pertaining to the disturbance were located between latitude 22° and 27° moving with a range of velocities of 100 to 125 m s^{-1}. In general, these values are well below the preeruption wind profile, a situation also observed in 2007 [*Sánchez-Lavega et al.*, 2008]. The dispersion in the wind speeds is very high, reaching up to 50 m s^{-1} in a given latitude, well above the uncertainties of the measurement. A mean value for the wind speed dispersion is about 20 m s^{-1} within the cyclonic latitude band from 24° to 26°. These motions indicate that the cloud features are not acting as passive tracers of the flow but that local motions generated by turbulence and waves in the wake of the plumes are involved. In fact, this latitude band is where the preeruption wind profile satisfies the necessary but not sufficient condition for barotropic instability [e.g., *Pedlosky*, 1979]. According to the Rayleigh-Kuo criterion, this implies that $\beta - \frac{d^2u}{dy^2}$ changes sign in the domain (Figure S6). Here $\beta = \frac{2\Omega \cos\varphi}{R}$ is the meridional gradient of the Coriolis parameter $f = 2\Omega \sin\varphi$ at latitude φ, where Ω is the planetary rotation rate (SIII for Jupiter), u is the mean zonal velocity, y is the meridional coordinate, and R is the planet radius.

There is no evidence that the large differences in the velocity field are due to altitude effects (i.e., tracers at different altitude coupled to vertical wind shears) since the same red wavelengths were used for the tracking before and during the disturbance development.

4. Dynamical Numerical Modeling

We have employed two dynamical models to simulate the observed cloud field and motions of the NTBD: a shallow water (SW) model [*Legarreta et al.*, 2016; *García-Melendo and Sánchez-Lavega*, 2017] and the Explicit

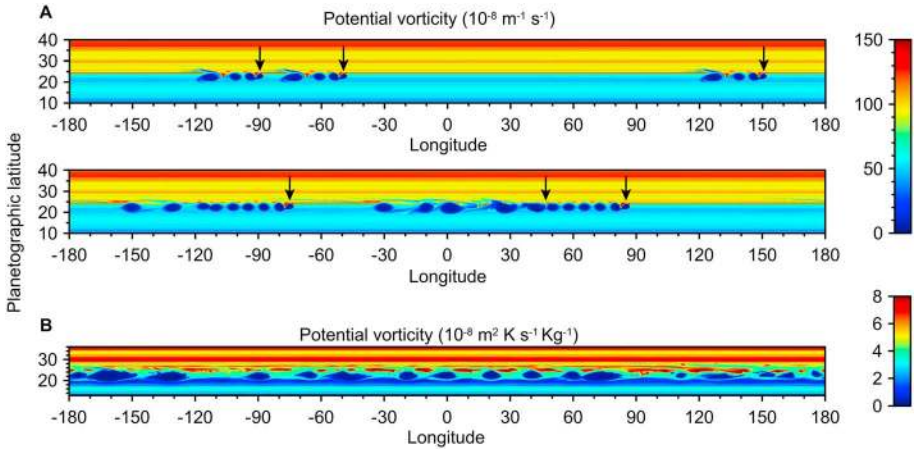

Figure 5. Numerical simulations of the NTBD using three sources as plumes: (a) Shallow Water model (potential vorticity (vorticity/thickness) and (b) EPIC model (Ertel potential vorticity [*Sánchez-Lavega*, 2011]. The upper panel identifies the plumes by arrows and shows the evolution of the NTBD after 7 and 18 days, respectively. The bottom panel shows EPIC results after 45 simulation days of the three-plume evolution.

Planetary Isentropic-Coordinate (EPIC) general circulation model [*Dowling et al*., 1998; *García-Melendo et al*., 2005]; see supporting information for details and *Sánchez-Lavega* [2011] for definitions.

In Figure 5 we show selected results of our simulations using both models when injecting three sources (each 1° in radius) placed at longitudes 0°, 40°, and 240°. Results are sensitive to the latitude where the perturbation is injected. The SW model is able to reproduce the periodic pattern in the wake of the plumes when the initial disturbance is located in the latitude range 24.5° to 25°. Out of these latitudes results diverged from the observed morphology. For the three sources we find the best simulated cases to occur for Rossby deformation radius $L_D \sim 1000$ km and an altitude of the disturbed surface 1/20 the thickness of the SW layer. The EPIC model gives us information on the possible vertical structure of the atmosphere just before the storm outbreak. The simulations that best reproduce the observations occur when the zonal wind has no vertical shear beneath the upper clouds and the Brunt-Väisälä frequency is set at $N \sim 5 \times 10^{-3}$ s^{-1}. Both the SW and EPIC models require that the sources must be located at 24.5°N. This suggests that the plumes have their base at a latitude different than observed, and therefore, the ascending mass flow should be tilted meridionally with respect to the local vertical and, as observed, moving faster than the velocities implied by the jet profile. From the dynamical point of view, both models are able to reproduce the general periodic patterns, suggesting that they are generated by the divergence of upwelling material transported aloft by the convective activity close to the tropopause, the injection of relative vorticity, and its interaction with the jet peak at 23.5°. Both models are unable to reproduce some more specific details such as the arcs displayed in Figure 3c.

5. Discussion

The SEBD and NTBD planetary-scale disturbances represent one of the major challenges to understand Jupiter's atmospheric dynamics, but at the same time the underlying physics can give us important insights into the parameters that define the upper troposphere, beneath the upper clouds, such as the abundance of water needed to initiate moist convection and the vertical structure of winds and temperature. They are also important because they give us information about the nature of Jupiter's winds through the turbulence pattern the plumes generate in their wake (vortices, swirls, filaments, and waves) and on how they transfer or extract energy and momentum from or to the zonal flow, changing the wind profile as reported in this paper [*Sánchez-Lavega et al*., 2008; *Barrado-Izagirre et al*., 2009].

There are some aspects of the disturbances that are mysterious: Why are they cyclical and what process establishes the temporal scale between events? What is the subjacent trigger mechanism? Why is there a fixed latitude for the convective plumes and why a variable number of sources (one, two, and four in different historical events observed so far)? Because this eruption occurred less than a month after Juno's perijove-1

PJ1 passage, analysis of the data provided at that time by instruments probing Jupiter's troposphere can give important information about the origin of this disturbance, for example, the presence of anomalies in the temperature or compositional properties at the latitude of the jet. The same analysis of both Juno and Earth-based supporting observations following perijove-3 on 11 December, i.e., when the plumes have ceased and the mixing in the latitude band has formed the reddish belt, will provide information on the perturbations the disturbance has produced.

Acknowledgments

This work was supported by the Spanish project AYA2015-65041-P with FEDER support, Grupos Gobierno Vasco IT-765-13, and by Universidad del País Vasco UPV/EHU through program UFI11/55. P.I. was supported by Aula EspaZio Gela under contract from Diputación Foral de Bizkaia. A portion of this research was supported by the National Aeronautics and Space Administration with funding both for the Juno Project and for the ground-based support at the Jet Propulsion Laboratory, California Institute of Technology. We thank all the observers who contributed to the PVOL2 database. A list of the database web addresses where the images used in this paper can be found is given in the supporting information (Text S1).

References

Barrado-Izagirre, N., S. Pérez-Hoyos, E. García-Melendo, and A. Sánchez-Lavega (2009), Evolution of the cloud field and wind structure of Jupiter's highest speed jet during a huge disturbance, *Astron. Astrophys.*, *507*, 513–522.

Dowling, T. E., A. S. Fischer, P. J. Gierasch, J. Harrington, R. P. Lebeau, and C. M. Santori (1998), The Explicit Planetary Isentropic-Coordinate (EPIC) Atmospheric Model, *Icarus*, *132*, 221–238, doi:10.1006/icar.1998.5917.

García-Melendo, E., A. Sánchez-Lavega, and T. E. Dowling (2005), Jupiter's 24°N highest speed jet: Vertical structure deduced from nonlinear simulations of a large amplitude natural disturbance, *Icarus*, *176*, 272–282.

García-Melendo, E., and A. Sánchez-Lavega (2017), Shallow water simulations of the three last Saturn's giant storms, *Icarus*, *286*, 241–260.

Hansen, C. J., M. A. Caplinger, A. Ingersoll, M. A. Ravine, E. Jensen, S. Bolton, and G. Orton (2014), JunoCam: Juno's outreach camera, *Space Sci. Rev.*, doi:10.1007/s11214-014-0079-x.

Hueso, R., J. Legarreta, E. García-Melendo, A. Sánchez-Lavega, and S. Pérez-Hoyos (2009), The Jovian anticyclone BA: II. Circulation and interaction with the zonal jets, *Icarus*, *203*, 499–515.

Hueso, R., J. Legarreta, S. Pérez-Hoyos, J. F. Rojas, A. Sánchez-Lavega, and A. Morgado (2010), The international outer planets watch atmospheres node database of giant planets images, *Planet. Space Sci.*, *58*, 1152–1159.

Hueso R., J. Juaristi, J. Legarreta, A. Sánchez-Lavega, J. F. Rojas, S. Erard, B. Cecconi, and P. Le Sidaner (2017a), The Planetary Virtual Observatory and Laboratory (PVOL) and its integration into the Virtual European Solar and Planetary Access (VESSPA), *Planet. Space Sci.*, doi:10.1016/j.pss.2017.03.014, in press.

Hueso, R., et al. (2017b), Jupiter cloud morphology and zonal winds from ground-based observations before and during Juno first perijove, *Geophys. Res. Lett.*, 44, doi:10.1002/2017GL073444, in press.

Irwin, P. G. J. (2003), *Giant Planets of Our Solar System*, pp. 197–246, Springer & Praxis, Chichester, U. K.

Karkoschka, E., and M. G. Tomasko (2010), Methane absorption coefficients for the Jovian planets from laboratory, Huygens, and HST data, *Icarus*, *205*, 674–694.

Legarreta, J., N. Barrado-Izagirre, E. García-Melendo, A. Sánchez-Lavega, J. M. Gómez-Forrellad, and the IOPW team (2016), A large active wave trapped in Jupiter's equator, *Astron. Astrophys.*, *586*, 9, doi:10.1051/0004-6361/201526197.

Mendikoa I., A. Sánchez-Lavega, S. Pérez-Hoyos, R. Hueso, J. F. Rojas, J. Aceituno, F. Aceituno, G. Murga, L. de Bilbao, and E. García-Melendo (2016), PlanetCam UPV/EHU: A two channel lucky imaging camera for solar system studies in the spectral range 0.38–1.7 microns, *Publ. Astron. Soc. Pac.*, *128*, 035002.

Pedlosky, J. (1979), *Geophysical Fluid Dynamics*, chap. 7, pp. 504–512, Springer, New York.

Peek, B. M. (1958), *The Planet Jupiter*, chap. 9, pp. 75–82, Faber & Faber, London.

Rogers, J., and H.-J. Mettig (2008), Jupiter in 2007: Final numerical report (British Astronomical Association). [Available at http://www.britastro.org/jupiter/2007report20.htm.]

Rogers, J. H. (1976), A high-velocity outbreak on the North Temperate Belt, *J. Br. Astron. Assoc.*, *86*, 401–408.

Rogers, J. H. (1992), Jupiter in 1989-90, *J. Br. Astron. Assoc.*, *102*, 135–150.

Rogers, J. H. (1995), *The Giant Planet Jupiter*, chap. 7, pp. 101–110, Cambridge Univ. Press, Cambridge, U. K.

Rogers, J. H., H.-J. Mettig, and D. Peach (2006), Renewed acceleration of the 24°N jet on Jupiter, *Icarus*, *184*, 452–459.

Rogers, J. H. (2016), Start of the 2016 NTBs outbreak. Jupiter in 2016/17: Report no.1, British Astronomical Association. [Available at https://www.britastro.org/node/8102.]

Rogers J. H., and G. Adamoli (2012), Progress of Jupiter's great northern upheaval, 2012 July–August, Jupiter in 2012/13: Interim report no. 3 (British Astronomical Association). [Available at http://www.britastro.org/jupiter/2012_13report03.htm.]

Sánchez-Lavega, A. (2011), *An Introduction to Planetary Atmospheres*, chap. 7, pp. 353–427, Taylor-Francis, CRC Press, Florida.

Sánchez-Lavega, A., and J. M. Gómez (1996), The South Equatorial Belt of Jupiter. I: Its life cycle, *Icarus*, *121*, 1–17.

Sánchez-Lavega, A., and J. A. Quesada (1988), Ground-based imaging of Jovian cloud morphologies and motions: II. The northern hemisphere from 1975 to 1985, *Icarus*, *76*, 533–557.

Sánchez-Lavega, A., I. Miyazaki, D. Parker, P. Laques, and J. Lecacheux (1991), A disturbance in Jupiter's high-speed north temperate jet during 1990, *Icarus*, *94*, 92–97.

Sánchez-Lavega, A., et al. (2008), Depth of a strong Jovian jet from a planetary-scale disturbance driven by storms, *Nature*, *451*, 437–440.

Sánchez-Lavega, A., S. Pérez-Hoyos, R. Hueso, T. del Río-Gaztelurrutia, and A. Oleaga (2014), The Aula EspaZio Gela and the Master of Space Science and Technology in the Universidad del País Vasco (University of the Basque Country), *Eur. J. Eng. Educ.*, *39*, 518–526.

Sánchez-Lavega, A, G. Fisher, L. N. Fletcher, E. García-Melendo, B. Hesman, S. Pérez-Hoyos, K. Sayanagi, and L. A. Sromovsky (2017), The great Saturn storm of 2010–2011, in *Saturn in the 21st Century*, chap. 13, Cambridge Univ. Press, Cambridge, U. K., in press. [Available at arXiv 1611.07669.]

Simon, A. A., M. H. Wong, and G. S. Orton (2015), First results from the Hubble OPAL program: Jupiter in 2015, *Astrophys. J. Lett.*, 812–855.